

# Speed and Current Control of a Permanent-Magnet DC Servo Motor Using a Real-Time Microcontroller

Julio Noel Hernández-Pérez, Jesús Ebert Giral-Salas, Roberto Morales-Caporal, Rafael Ordoñez-Flores  
and Miguel Ángel Morales-Flores

División de Estudios de Posgrado e Investigación, Insituto Tecnológico de Apizaco  
Av. Instituto Tecnológico S/N, Col. Centro. C.P. 90300. Apizaco, Tlaxcala. México  
e-mails: juli11060986@hotmail.com; ebgiral@hotmail.com; rmcaporal@ieee.org

**Abstract**—This paper presents the digital implementation of a double-loop feedback controller for speed and current regulation on a permanent-magnet direct current servo motor based on the real-time microcontroller TMS320F28335. The topology of the controller is based on a cascade control scheme; the speed controller (external loop) sets the reference of the current controller (internal loop). In this way, a high performance on the servo drive can be obtained. A online tuned Proportional-Integral controller regulates the speed reference, the armature current is regulated using a hysteresis controller. In order to make comparisons a single topology speed controller (one control loop) and cascade topology speed and current controllers (double control loop) are digitally implemented. Simulation results are validated by practical experimentation. Electrical drive and sensor platform were developed for the tests. Additionally a data acquisition system is proposed.

**Keywords**—Current control, direct current, real time, permanent magnet, servo motor, speed control.

## I. INTRODUCTION

The permanent-magnet direct current servo motors (DCSM) are highly used in industrial and home applications such as: machine tools, presses, coiling, robotics, manipulators, wheelchair, treadmills, etc; where high-performance speed and torque control are required [1], [2].

This kind of machine has no external winding, so that, their structure is smaller than a machine with field winding of the same power. The biggest disadvantage of the DCSM is the possibility of demagnetization of the magnet, particularly when over-heating is developed by overloading the machine for prolonged periods of time, fortunately new materials are being developed [3].

In electric traction, like in other applications, a wide range of speed and torque with high performance is desired. The brushed DC motor with field winding fulfills these requirements, although this machine needs periodic maintenance and a second voltage source. The DCSM does not require a second voltage source, which increases its reliability, its power-to-weight ratio and its efficiency. Moreover, DCSM play a fundamental role in robotics and automation. Fast dynamical response, high torque to weight ratio and linear dependence of the torque on the current constitutes the most interesting features of this kind of servo motors [4], [5].

On the other hand, the classical control theory presents a low cost response for practical applications of the servo. Classical control strategies like Proportional-Integral (PI) generate high performance responses under different kinds of industrial processes; if the strategy is implemented in multi-control loops, it has the ability to eliminate steady state offsets [6], [7].

Willing to obtain a better performance, a cascade controller has been implemented. When significant dynamics exists this is particularly useful, e.g., long dead times or long time constants, between the control and the process variables. Tighter control can then be achieved by using an intermediate measuring signal which responds faster than the controlled signal [8].

The conventional linear control-system design for permanent-magnet DCSM drives consists in a properly tuned cascade configuration of PI speed and torque controllers. Rather accurate information regarding the motor parameters and load conditions is necessary to guarantee the desired tradeoff between precision, bandwidth, and disturbance rejection [8].

This work is focused on the design and implementation of speed feedback control; which can regulate the rotor speed relative to a reference velocity even if a disturbance, such as external changes of the load torque, is placed.

First the mathematical model of the DCSM was developed, then the single and cascade schemes were proposed; then the closed-loop scheme was designed and simulated using Matlab/Simulink®.

Results were confirmed via experiments. Power electronics and sensor stages required for activation of the proposed system with scheduling control techniques were designed and built in the laboratory; the digital platform and the permanent-magnet DCSM were purchased.

## II. SYSTEM MODELLING

### A. Electrical model

Fig. 1 shows a basic electrical scheme of the permanent-magnet DCSM [3]. By analysis of Kirchhoff:

$$V_a = R_a i_a + L_a (di_a/dt) + e_a \quad (1)$$

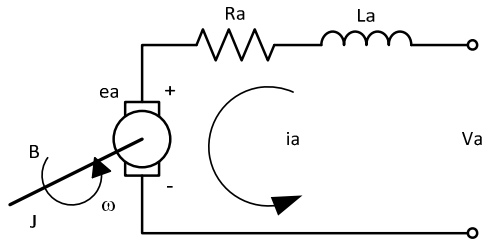


Fig. 1 Basic scheme of the permanent-magnet DCSM

Where  $V_a$  is the armature voltage.  $R_a$  and  $L_a$  are armature resistance and inductance,  $i_a$  is the armature current and  $e_a$  is the electromotive force (EMF).

By properties of the machine:

$$e_a = K_b \omega \quad (2)$$

$K_b$  represents the electric constant and  $\omega$  is the angular velocity of the rotor. By using the equation (1) and (2) and solving the derivate of the current:

$$(di_a/dt) = (1/L_a)(V_a - R_a i_a - K_b \omega) \quad (3)$$

#### B. Mechanical Model

By Newton's mechanical equilibrium law the mechanical model of the machine is described as:

$$\tau_e = J(d\omega/dt) + B\omega(t) + \tau_L \quad (4)$$

Where  $\tau_e$  is the electromechanical torque,  $J$  is the inertia of the machine,  $B$  is the viscosity coefficient and  $\tau_L$  is the torque constant of DCSM.

By properties of the machine:

$$\tau_e = K_m i_a \quad (5)$$

$K_m$  represents the mechanical constant. By using equations (4) and (5), sets  $B \approx 0$  and solving for derivate of speed:

$$(d\omega/dt) = (1/J)(K_m i_a - \tau_L) \quad (6)$$

Equations (3) and (6) show the dependence between each other, a double feedback control scheme must be implemented at the same time for both variables to improve the response of the system.

### III. CONTROL SYSTEM DESIGN

A cascade control scheme was proposed according to regulate rotor speed and armature current; this scheme consist in two feedback control loops, the first one (external loop) for speed and the second one (internal loop) for current [7]. The selected strategies for the cascade scheme are: the Proportional-Integral control for the speed, and the Hysteresis control for the current [8].

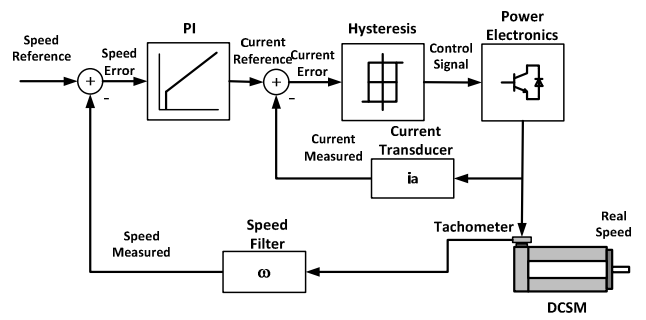


Fig. 2 Block diagram of the used control Strategy.

#### A. PI Control

The PI Control strategy is one of the most common used algorithms in feedback control applications. General PI algorithm is described in the following equations [7], [9]:

$$u(t) = K[e(t) + (1/T_i) \int e(t) dt] \quad (7)$$

Where  $u(t)$  is the output value of the control algorithm,  $K$  is the proportional factor of the PI and  $T_i$  is integral time; measurement error  $e(t)$  is achieved by comparing the reference value (RV) against the measured value (MV). The system variable  $e(t)$  will be subsequently used by the change algorithm PI control system.

$$e(t) = RV - MV \quad (8)$$

PI implements a proportional factor ( $K$ ) to the error measured at each sampling period, while the integral stage is obtained integrating the error at all times using the integral constant  $K_i$ . The following equations show the development of the proportional and integral stages:

$$P = K e(t) \quad (9)$$

$$I = K_i \int e(t) dt \quad (10)$$

Where  $K_i = K/T_i$ . Using (9) and (10), (7) can be simplified as:

$$u(t) = P + I \quad (11)$$

The PI algorithm generates a real output control, in this case for the speed. The output is scaled at 0-100%; an adjusted value is needed for a single PI implementation because the output value cannot be placed directly in the digital algorithm.

#### B. Hysteresis Control

The hysteresis control is the most basically feedback control strategy. Its operation can be described by a simple switch which changes its state from the behavior of the process value in a hysteresis band [9].

When the value of the input exceeds a reference value ( $+U$ ), the output interrupt changes its state to *off mode*; when the input value is less than a reference value ( $-U$ ) the interrupt state changes to *on mode*; while the value of the input variable

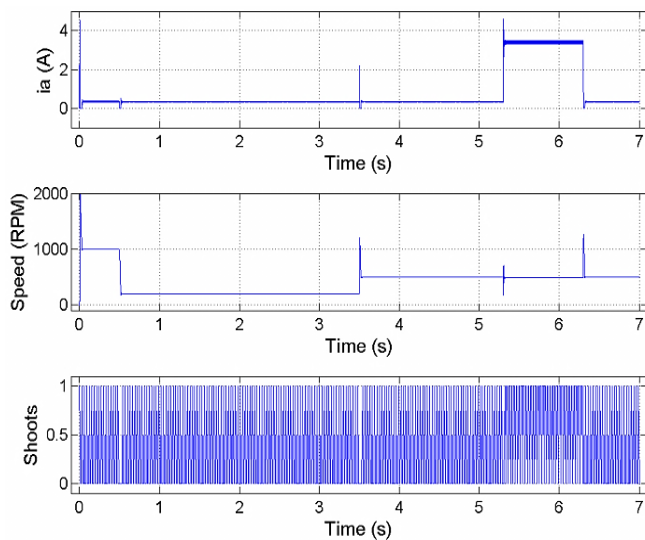


Fig. 3 Simulated results of single PI control scheme for the permanent-magnet DCSM

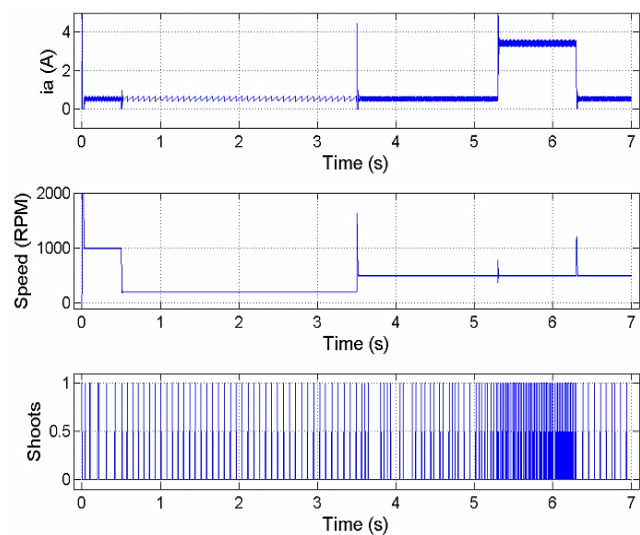


Fig. 4 Simulated results of cascade control (double-loop) scheme for the permanent-magnet DCSM

stays between a desired value of the hysteresis band  $(-U, +U)$ , the interrupt does not change the present mode.

### C. Cascade Control Scheme(PI/Hysteresis)

The cascade control complements the control system to place the best features of the two selected strategies (PI/Hysteresis). The PI algorithm gets the measured speed error and generates an output value (armature current reference) which is arithmetically added to the measured current, then the current error feeds the hysteresis algorithm. The algorithm processes the information and generates an output control value (0,1) in order to fire the power transistor which will drive the permanent-magnet DCSM as shown in Fig 2.

## IV. SIMULATED RESULTS

Two control schemes have been programmed for comparison purposes, a single PI control scheme and a cascade control scheme. The platform used for simulations is Matlab/Simulink®. For the single PI scheme, current control is suppressed. The response of the servo motor for single control (speed) and for the double control loop (speed and current) are shown in Fig. 3 and 4 respectively.

The changes in the speed reference are placed at the following times: [0 s - 1000 RPM], [0.5 s - 200RPM] and [3.5 s - 500RPM]; while disturbance in the load torque occurs at the instant 5.2s and finish at 6.3s, it is to be noticed that a load torque disturbance (equivalent to 3.5A) is placed because in a real implementation the measuring the torque implies the use of other measuring device and then a bigger costs.

The single PI scheme has an acceptable response in relation to the load disturbances showing only a small overshoot when the load torque is placed and released.

The cascade strategy presents a high switching frequency response when speed and torque disturbances are introduced, the current ripple increases significantly more than the single PI scheme.

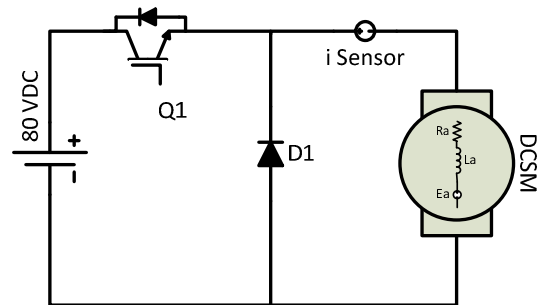


Fig. 5 Power electronics diagram for the main test

## V. EXPERIMENTAL RESULTS

### A. Power Electronics

The implemented power electronics diagram is shown in Fig. 5. It is composed by an Isolated Gate Bipolar Transistor (IGBT), the IGBT is being switched through the drive HCPL316J and a high speed power diode in parallel with the DCSM.

The DC voltage source is set to 80 V. The switching signal is generated in the programmed control strategy in the real-time Microcontroller. A Hall Effect sensor (LTS25:  $\pm 27A$ , 0.625V/8A) is used for measuring current. The rotor speed signal is sensed via a tachometer placed inside the servo motor; this signal is also filtered and adjusted. These measured signals had to be pre-adjusted prior to being measured by the Microcontroller, Fig. 6 shows the prototype assembled in the laboratory.

### B. Commercial DC Motor

The permanent-magnet DCSM used is a Baldor DC Servomotor model: MT-3353-BLYAN. The features described by the manufacturer are showed in Table I. The rotor speed is verified via a mechanical tachometer, whit this information the rotor speed is classified as linear when rise and fall of speed occurs.

TABLE I  
PERMANENT-MAGNET DCSM FEATURES

Features	Value
Max. voltage	120 $V_{CD}$
Rated voltage	100 $V_{CD}$
Armature resistance	5.6 $\Omega$
Armature inductance	15.5 mH
Electric constant	30.7 V/KRPM
Max Speed	4 KRPM
Rated Speed	2.8 KRPM
Inertia	1.84 Kg-cm <sup>2</sup>
Mechanical constant	0.29 Nm/A
Torque constant	0.71 Nm
Tachometer	10 V/1.4 KRPM



Fig. 6 Laboratory test prototype, a) DCSM used, b) personal computer (PC), c) digital platform, d) speed signal filter, e) power electronics, f) current sensor

### C. Digital Platform

The selected device to implement the control algorithm is the real-time Microcontroller TMS320F28335 [10]. It processes the data information coming from the DCSM, activating the power electronics and at the same generates the data acquisition stage. It has 32-bit digital signal processor (DSP) architecture, and advanced control peripherals.

This kind of digital platform allow the implementation of different control technics which require high execution speed per iteration as used in this work in reference with the hysteresis band weight in the cascade control scheme.

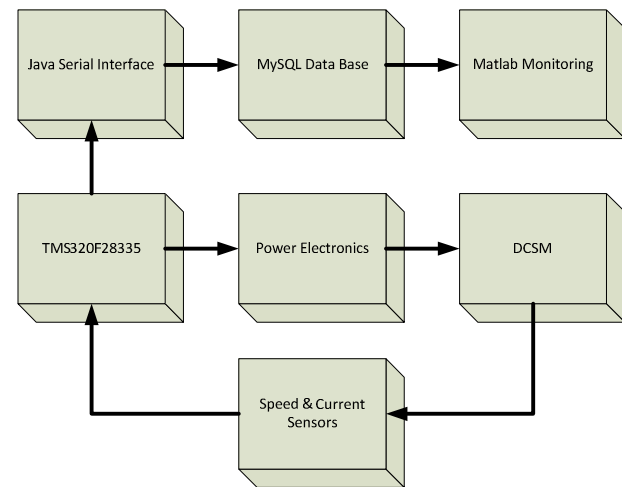


Fig. 7 Data acquisition block diagram

Fig. 6c shows the digital platform used, wired to the power electronics and connected to a personal computer (PC). The selected control algorithms do not represent greater complexity, however its implementation on a digital platform does. This device can be programed in C language through the Code Composer Studio® (CCS) compiler; which gives the possibility to develop algorithms more easily; that would be very complicated to implement on assembly language.

The Microcontroller has the following features, whose describe the operation of the digital platform and the routines which can be programmed:

- 150MHz - Process frequency
- 6.67ns - Instruction time per cycle
- Float point unit
- 256 Kb - Flash memory
- 34Kb - RAM memory
- 1Kb - ROM memory
- PWM outputs
- High resolution PWM outputs
- Quadrature encoder channels
- Analog/Digital converters
- TTL low voltage technology
- 88 I/O general propose
- Serial communication interface

### D. Data acquisition

For digital visualization purposes of the performance of the permanent-magnet DCSM, a data acquisition stage was implemented in the digital platform. Every 14ms, a data package (time, speed, current and shoots) is saved in an array; each packet has a length of 500 slots.

When the control routine is over, data sending is started. Using the Serial Communication Interface (SCI) [11] in the Microcontroller, one by one, each packet is encoded into a character string. SCI is programmed to send data in 9600 bauds/s. Data is sent and decoded by a Java® program, recorded in an external MySQL® database and after read by a



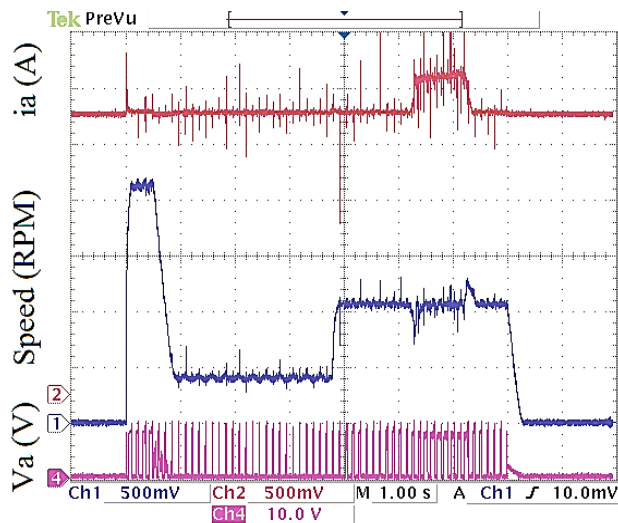


Fig. 8 Scope monitoring for single PI control scheme in DCSM

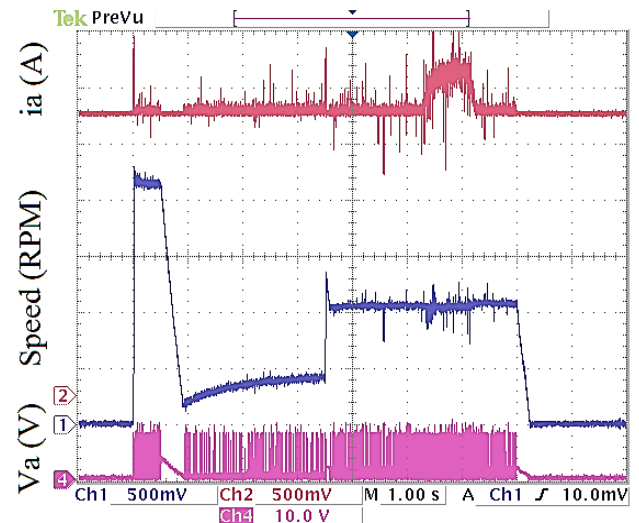


Fig. 9 Scope monitoring for cascade control scheme in DCSM

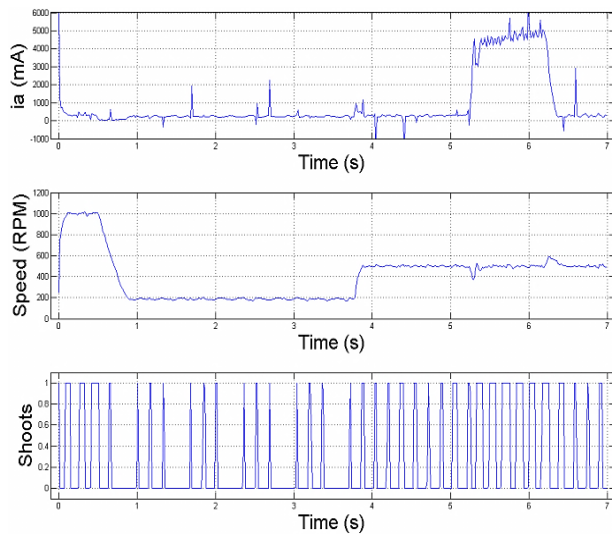


Fig. 10 Data acquisition for single PI control scheme in DCSM

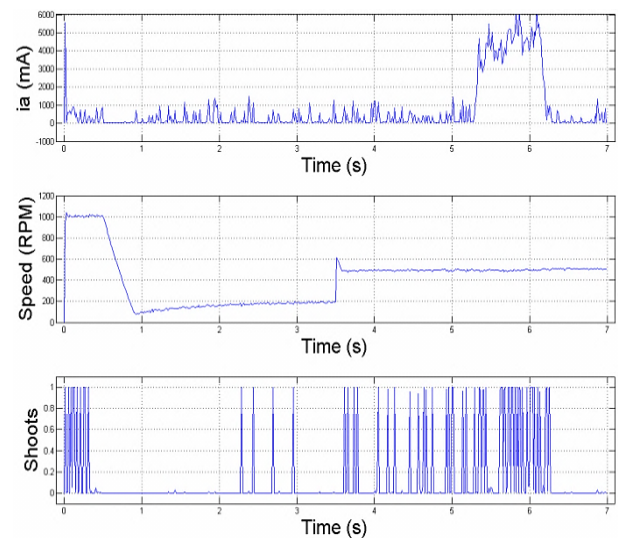


Fig. 11 Data acquisition for cascade control scheme in DCSM

Matlab® program, Fig. 7 shows the block diagram for the data acquisition.

### E. Laboratory Test

The cascade control scheme for speed and current is obtained by programming the equations (7)-(11) and implementing the concept of Fig. 2.

PI algorithm is online tuned for both schemes [7], [8]; the proposed gains are:  $K_p = 1$ ,  $K_i = 0.5$  for the single PI scheme and  $K_p = 0.8$ ,  $K_i = 0.01$  and 10% of hysteresis band for the cascade scheme. The correct tuning of PI algorithm offers output signals with high performance response to the disturbance in DCSM [12]. Figs. 8 and 9 show the analog results via oscilloscope measurements for the single PI and cascade scheme respectively. Figs. 10 and 11 show the digital results via data acquisition for the single PI and cascade scheme respectively. Mentioned above armature current, rotor speed and digital gate signals are shown at the top, the middle and bottom of the figures respectively.

The rotor speed changes and torque disturbance are programmed in the digital platform, Table II show them. It is to be noted that the engine speed decreases slowly when going from high to low reference speed; this is due to the absence of an electric brake in the design. At the single PI scheme, rotor speed reference is reached in a perceptible transient time in all the speed changes. Small oscillations are observed during steady state of signals speed.

Although speed references are reached during operation, significant speed changes are observed when applying or removing an external load torque. The armature current presents a lot of disturbances as positive and negative peaks in all the operation time, particularly when the machine starts and the load torque is applied or removed. The single PI offers a constant 15 KHz frequency; nevertheless speed and disturbance performances are not good.

In the other case, the cascade scheme presents a better response during speed changes and insignificant losses by load torque disturbances. Unfortunately current ripple increases, this

TABLE II  
DISTURBANCES PROGRAMED ON THE PERMANENT-MAGNET DCSM

Time (s)	Rotor Speed (RPM)	Load disturbance (A)
0	0	X
0 - 0.5	1000	X
0.5 - 3.5	200	X
3.5 - 7	500	X
5.2 - 6.3	500	5

caused by the hysteresis algorithm, which sets the switching frequency as not constant; this makes necessary the use of faster electronics.

## VI. CONCLUSION

The cascade control scheme presents a better performance compared to the single PI scheme during speed and load torque changes as shown in the simulations.

The cascade scheme works under variable frequency regimen, therefore power electronic devices are always under stress due to constant frequency changes that is why the use of robust electronics is necessary.

Although the cascade scheme scheduling algorithm does not has a significant complexity, the variable frequency regimen affects likewise the switching operation on the digital platform which means the use of a high resolution digital system as presented is needed.

Using the data acquisition system a better visualization of the system response can be presented, it reflexes a better perspective of the rotor speed and stator current. Nevertheless the sampling time reduces the signal resolution and bandwidth. The use a high performance DSP would reduce the sampling time and obtain a bigger data buffer for data visualization. The data collected can be used as a basis for the implementation of intelligent control algorithms.

## REFERENCES

- [1] R. Morales Caporal, I. Hernández Dávila, E. Bonilla Huerta and J. C. Hernández Hernández, "speed and position control of a direct current motor using fuzzy logic and artificial neural networks (in Spanish)," *IX Congreso Internacional Sobre Innovación y Desarrollo Tecnológico (CIINDET'11)*, Cuernavaca, México, November 2011, Paper 636.
- [2] R. Morales Caporal, J. I. Paredes Tabales, O. Sandre Hernández, E. Bonilla Huerta and J. F. Ramirez Cruz, "Application of intelligent control techniques in a direct current motor including pulse-width modulation (in Spanish)," *Research in Computing Science (RCS)*, October 2012. Vol. 60. pp. 121-130.
- [3] A. E. Fitzgerald, C. Kingsley Jr y S. Umans., *Máquinas Eléctricas*, McGraw Hill.
- [4] J. Dixon, M. Rodríguez y R. Huerta, Position Estimator and Simplified Current Control Strategy for Brushless-DC Motors, Using DSP Technology, *IECON 02*, 2002
- [5] C. Rossi y A. Tonielli, Robust Control of Permanent Magnet Motors: VSS Techniques Lead to Simple Hardware Implementations, *IEEE Transactions on Industrial Electronics*, vol. 41, n° 4, pp. 451-560, 1994.
- [6] K. Ogata, *Ingeniería de Control Moderna*, Pearson Education.
- [7] K. J. Aström y T. Hägglund, *PID Controllers*, 2nd Edition, Instruments Society of america, 1995.
- [8] A. Pisano, A. Davila, L. Fridman y E. Usai, Cascade Control of PM DC Drives Via Second-Order Sliding-Mode Technique, *IEEE Transactions on Industrial Electronics*, vol. 55, n° 11, pp. 3846-3854, 2008.
- [9] B. C. Kuo, *Sistemas de control Automático*, Prentice Hall, 1996.
- [10] T. Instruments, «Texas Instruments,» [En línea]. Available: <http://www.ti.com/product/tms320f28335>. [Last acces: 05 30 2013].
- [11] T. Instruments, «Texas Instruments,» [En línea]. Available: <http://www.ti.com/lit/ug/sprufz5a/sprufz5a.pdf>. [Último acceso: 30 05 2013].
- [12] N. Ozturk, «Speed Control for DC Motor Drive based on Fuzzy and Genetic PI Controller - A Comparative Study,» *Electronics and Electrical Engineering*, n° 7, pp. 43-48, 2012/.